A Functional In Vitro Model for Studies of Intracellular Motility in Digitonin-permeabilized Erythrophores

MARK E. STEARNS and ROBERT L. OCHS

Department of Molecular, Cellular, and Developmental Biology, University of Colorado at Boulder, Boulder, Colorado 80309. Dr. Ochs's present address is the Department of Pharmacology, Baylor College of Medicine, Houston, Texas 77030.

ABSTRACT Phase contrast cine results demonstrate that erythrophores maintain saltatory particle motion for hours after permeabilization with 0.001% digitonin in a cytoskeletal stabilizing solution at 23°C. High voltage electron microscopy (HVEM) studies reveal that cytoskeletal elements are retained intact, except in immediate subplasmalemmal regions where the plasma membrane is punctured by digitonin. During digitonin treatments, cells are permeable to ions, small molecules, and antibodies. We find that motion is Ca^{2+} and ATP-sensitive, and optimal in PIPES buffer (pH 7.2) containing 1 mM Mg^{2+}/ATP and EGTA-Ca^{2+} (10^{-7} M Ca^{2+}) at 37°C. Experiments testing the inhibitory effects of vanadate (0.4–10 μM), ouabain (100–600 μM), *N*-ethyl maleimide, and the cytochalasins B and D indicate that a dyneinlike ATPase may provide the motive force for driving saltatory pigment motion in erythrophores.

The cyclic aggregation and dispersion of pigment granules in fish chromatophores provides an ideal system for studies of intracellular motility. The appeal of the chromatophore system resides with the fact that two types of particle motion occur in this cell, a nonsaltatory, uniform movement during pigment aggregation (25), and a saltatory motion during pigment granule dispersion (25). The cytoplasmic processes governing these movements of pigment granules are only beginning to be understood.

Morphological evidence and studies of the effects of antimicrotubule agents on pigment migration have demonstrated that numerous radially arrayed microtubules are important, at least in establishing the direction of pigment translocations (1, 4, 21, 25, 29, 36). In addition, thin section work on erythrophores (25) and on melanophores (32) has shown that microtubules disassemble, in part, with each aggregation and that they reassemble during dispersion. The significance of this phenomenon to pigment motion is not clear.

Green (18) first proposed that pigment granules behave as if they are embedded in an elastic gel that "contracts" during pigment aggregation and "expands" during pigment dispersion. The structural properties and interactions of this matrix with pigment were later made clear in morphological studies on chromatophores. Based on stereo high voltage electron microscope (HVEM) images of melanophores and erythrophores, Porter and colleagues (4, 21), and Schliwa (29, 32) described a gel consisting of a latticework of cross-linking filaments, termed microtrabeculae, in which microtubules and pigment are suspended. HVEM observations at various phases of pigment translocation suggested an involvement of these microtrabeculae in the processes of granule movement (4, 21). Indeed, during pigment aggregation and dispersion, the microtrabecular lattice undergoes organizational transformations interpreted to be contractions and expansions of lattice filaments important for pigment motion (4, 21).

Stossel and Hartwig (34) and others have reported that myosin is involved in cytoplasmic gel contractions in diverse cell systems. Thus, some coincidence of content and behavior in the cytoplasmic matrix of chromatophores is possible though no convincing evidence has yet emerged to directly support such conjectures.

Elucidation of the force generating mechanisms regulating the two types of particle motion in model erythrophore systems is important and may be possible from immunochemical and biochemical studies. In this regard, Obika, et al. (22) have demonstrated an extensive network of actin microfilaments in fish melanophores which they presume is important for pigment translocations. Based on electron microscopy and immunofluorescent techniques, Schliwa, et al. (31) have found a subplasmalemmal network of actin in angelfish melanophores, but no actin filaments are reported in association with radial arrayed microtubules or with pigment in central motile areas of the cell. Further, stress fibers and microfilament bundles are not observed in melanophores or erythrophores indicating, in contrast to Obika's results, that actin is not directly involved in the processes of pigment motion.

THE JOURNAL OF CELL BIOLOGY · VOLUME 94 SEPTEMBER 1982 727-739

Our awareness of the complexities of microtubule directed motion could be benefited by the development of cell models for studying transport. Cande and colleagues (6, 7) have recently developed techniques for manipulating chromosome movements at anaphase in Brij-58 lysed mitotic spindles. They discovered that chromosome motion is ATP-requiring and is driven in part by a vanadate-sensitive dynein ATPase. This movement of chromosomes at anaphase is at a constant velocity, and is similar, except in rate, to the motion of aggregating pigment granules which suggests that both phenomena may involve identical mechanisms. Thus, the advantages of cell models in dissecting out components important for motility events has made it useful to develop permeabilized cell systems for investigating mechanisms of pigment translocation.

In this paper, we report methods for selectively permeabilizing the plasma membrane of cultured erythrophores using the cholesterol binding steroid glycoside, digitonin. These cells are readily permeable to agents ranging from divalent cations, nucleotides, and small molecules to antibodies. Using these models, buffer conditions adjusted for pH, Ca^{2+} ions, Mg^{2+}/ATP, and temperature have been determined for the maintenance, stopping, and reinitiation of saltatory transport in dispersed cells.

In this system the saltations of pigment parallel the saltatory action of chromosomes during early metaphase. Whether, in both instances, the motion is an expression of the action of a contractile component in the microtrabecular lattice (i.e., a dynein ATPase) is an intriguing possibility. We have investigated the effects of different drugs (vanadate, ouabain, cytochalasins, and *N*-ethyl moleimide [NEM]) which permit discrimination between the role of dynein and actomyosin contractile systems in cell motility events. The results indicate that dyneinlike ATPases provide the motive force for saltatory motion in erythrophores.

MATERIALS AND METHODS

Materials

Vanadate free ATP, and ADP were purchased from Boehringer-Mannheim Biochemicals, Indianapolis, IN. All other reagents were purchased from Sigma Chemical Company, St. Louis, MO. Anti-porcine HMW-MAPs have been previously characterized as specific for HMW-MAP 1 and 2 (11–13) and was a generous gift from Drs. Vitauts Kalnins and Joe Connolly, University of Toronto, Toronto, Canada. Antitubulin was a gift from Dr. Paul Burton, University of Kansas, Lawrence, KS, and was characterized as described in an earlier paper (23).

Cell Culture and Permeabilization Procedures

Erythrophores were isolated and cultured from scales of the squirrel fish, *Holocentrus ascensionis*, according to a modification (21) of the method described by Byers and Porter (4). After enzyme dissociation from the scale, cells were seeded onto either carbon-coated cover slips or onto Formvar and carbon-coated gold grids (21). Both cover slips and grids were glow-discharged with ionized aluminum to ensure attachment and spreading of the cells. Before permeabilization with digitonin, cells were routinely induced to disperse their pigment with 2.5 mM caffeine added to the culture medium. During permeabilization steps, cells attached to cover slips and grids were transferred to a slide for light microscopy observations. A thin layer of silicon grease on each side of the slide was used as a spacer and cover slips were placed on several drops of medium (cell side down) and sealed with Valap, leaving openings on each side for exchange of solutions. Cells were permeabilized with digitonin solutions by adding a drop on one side of the cover slip, waiting several minutes for solutions to equilibrate, then slowly removing ~1 drop from the other side with tissue paper. Five to ten changes of this type over about 3 min resulted in the permeabilization of 100% of the cells, although most cells were punctured within 10 s of exposure to digitonin.

In all these studies the behavior of cells was recorded by phase contrast cinematography (Zeiss Universal Microscope) at 120 frames/min and films analyzed with a stop motion projection from images projected sequentially on a 6-ft screen. The average rates of pigment motion were determined from five measurements of the distances moved by ten granules.

Electron Microscopy

For HVEM, cells plated on gold grids were fixed by addition of drops of 2.9% glutaraldehyde in Hank's balanced salt solution (HBSS) at 37°C for 30 min. Cells were then washed three times with HBSS, postfixed with osmium tetroxide for 2 min at 4°C, and washed with HBSS. After three rinses in distilled water, cells were dehydrated using a graded acetone series and dried by the critical-point method. Cells were lightly coated with layers of carbon and stored in a vacuum dessicator. Erythrophores were examined in the HVEM[1] under an accelerating voltage of 1,000 kV. This whole-cell fixation procedure is similar to that described previously by Wolosewick and Porter (37). The cells were lightly coated by vacuum evaporation of Pd/Au (6 mm) for examination of the plasma membrane in the HVEM.

Experimental Solutions

Solutions used in tissue culture and in the permeabilization experiments were sterilized by vacuum filtration through a 0.22-μm millipore filter (Millipore Corp., Bedford, MA). Precise Ca^{2+}/EGTA solutions with free Ca^{2+} ion levels (assumed KEca = $10^{7.08}$) in the range of 0.01 to 10 μM were prepared using a computer program written by John Gilkey that took into account the pH, the ionic strength, and Mg^{2+} ion concentration of the final solution. A stock solution of 100 μM vanadate was freshly prepared by solubilization in 0.1 M NaOH and appropriate aliquots added to experimental solutions. In vanadate studies, reversal was achieved by adding drops to cell solutions from a stock 100 mM pyrocatechol solution freshly prepared in 1 mM HCL, until ~1 mM levels were reached or, alternatively, vanadate was washed out with fresh buffer. Digitonin stock solutions at 0.4% were made in 50% ethanol and diluted to 0.001% in experimental solutions. Solution temperatures were maintained using a water bath and cells kept at a constant temperature using an air current incubator.

Antibody Experiments

With the exception of those shown in Figure 14, permeabilized cells were exposed to tubulin and HMW-MAPs antisera diluted 1:10 in permeabilization solutions for 30 min at 23°C. While still alive, these cells were then fixed by immersion in −20°C methanol, washed three times in phosphate buffered saline (PBS) pH 7.2 and incubated with fluorescein isothiocyanate (FITC) coupled to goat anti-rabbit (GAR) IgG (Miles Research) diluted 1:20 with PBS. After three rinses in PBS, the cells were mounted on slides with a mixture of 50% glycerol and 50% PBS, pH 7.8 and examined in a Leitz-Orthoplan microscope with epifluorescent illumination. Images were recorded on Tri-X film (ASA 400) and developed in diafine. In some studies (Fig. 18) cells were treated with permeabilization solutions and were then rapidly fixed by immersion in −20°C methanol, incubated with anti-tubulin (1:10 in PBS) followed by FITC (1:20 in PBS), and then prepared for light microscopy. Cells were washed three times with PBS between each of the above steps. The cell shown in Figure 14 was incubated in

[1] JEOL 1000 located at the Laboratory for High Voltage Microscopy, Boulder, CO, a resource facility supported by the National Institutes of Health.

FIGURE 1 Shows an erythrophore before (*a–d*) and after (*e–f*) permeabilization with digitonin. The cell shape and overall dispersed distribution pattern of pigment granules remains unchanged after permeabilization. The saltatory motion of individual granules (arrowheads) can be followed from *a* to *c* and *b* to *c*. *d* shows the cell immediately before detergent treatment. Saltations result in small changes in overall pigment distribution, and the cell is divided into quadrants intersecting at the cell center and an arrow marks the direction of motion of the granules indicated with arrowheads in each quadrant. The same cell is shown in Fig. 15 after 2 h in permeabilization buffer and after exposure to vanadate. × 2,500.

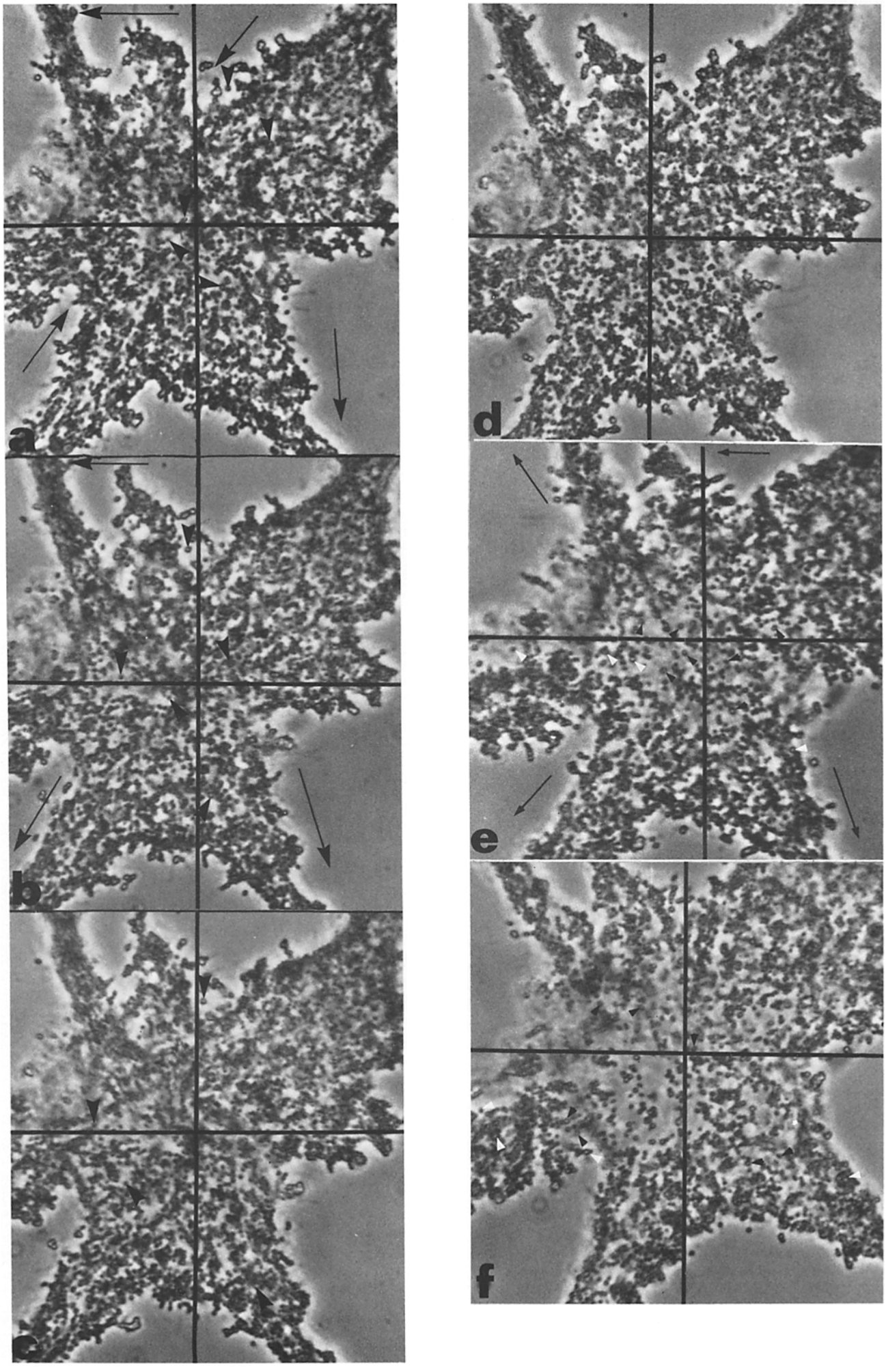
a
b
c
d
e
f

the presence of 10 μg/ml digitonin with tubulin antibody, washed three times by drawing 3 vol of fresh permeabilization buffer under the cover slip, incubated with Rhodamine isothiocyanate (RITC)-IgG, washed three times, and photographed using epifluorescent optics and rhodamine filters. After fluorescent imaging, the cell was examined by time-lapse microscopy to determine the extent of motion remaining in the cell. In the above studies, note that as much as 50% of the cells are lost during methanol fixation steps and about 50% of the cells retained exhibit no, poor, or diffuse fluorescent patterns.

RESULTS

Saltatory Transport in Permeabilized Cells

Fig. 1 *a–c* shows images printed from time-lapse cine records of a cultured erythrophore after caffeine treatment. The pigment granules are observed to exhibit a constant bidirectional saltatory motion to and from the cell center. With subsequent permeabilization using a 0.001% digitonin solution, 100% of the caffeine-treated cells maintain their shape and a uniformly dispersed pigment granule arrangement (Fig. 1 *d*). Some of the caffeine-dispersed granules remain in clusters at the cell periphery where they generally do not move unless the cell is stimulated to aggregate its pigment. After permeabilization with digitonin (Fig. 1 *d–f*) pigment continues to move bidirectionally from the cell center at rates approximating those observed for granules in intact cells (3–5 μm/s). Transport will continue for hours in these cells, although with time (1 h) the motion tends to become restricted to radially aligned regions of the cell which are divided by other regions where little or no transport occurs. In addition, granules will sometimes aggregate into small clumps of pigment which then move as a unit through the cytoplasm. One immediate clue that cells are being permeabilized in these experiments is the appearance of free-floating membrane vesicles due to digitonin-induced vesiculation of the plasma membrane. The linear motion of several of the granules (arrowheads) can be followed from Fig. 1 *e* to *f* taken at a 2-s interval.

An interesting bonus arising from stop-motion tracking of granule motion in these cells was that granules migrating away from the cell center tend to return to the same spot in the cell periphery from which they originated before beginning a new journey to the cell center (not shown). This behavior is probably a reflection of the highly ordered nature of the lattice matrix controlling pigment migration (26).

Attempts to induce cycles of aggregation and dispersion of pigment granules after permeabilization have been unsuccessful. Cells permeabilized without caffeine treatment respond by irreversibly aggregating their pigment. Cells permeabilized in the caffeine-dispersed state and then exposed to aggregating agents such as 100 mM KCl, or to solutions lacking caffeine, also aggregate their pigment and this effect is not countered with caffeine. Thus, all the results in this paper are reported on saltatory transport mechanisms in cells treated with 2.5 mM caffeine and permeabilized for <1 h.

Another indication of permeabilization is in part illustrated in studies of the effect of Ouabain on pigment distribution. Intact cells will normally respond to Ouabain (100 μM), a Na^+/K^+ ATPase inhibitor, to reversibly aggregate their pigment. Fig. 2 shows that permeabilized cells can no longer aggregate their pigment in the presence of Ouabain (100–600 μM) but will continue to exhibit saltatory motion, except when extremely high (toxic) amounts of Ouabain (1 mM) are applied.

Permeabilization Buffer

The composition of the permeabilization solution used is detailed in Table I. Digitonin used at 0.001% levels in this solution permits the gradual removal of plasma membrane components by 10–30 s. Figs. 3, 4, and 5 show that this treatment creates visible holes of various sizes in the plasma membrane of cultured erythrophores. The reader should compare Fig. 4 and 5 with Figs. 6 and 7 of a nonpermeabilized cell. HVEM images of metal-coated cells in Figs. 6 and 7 show

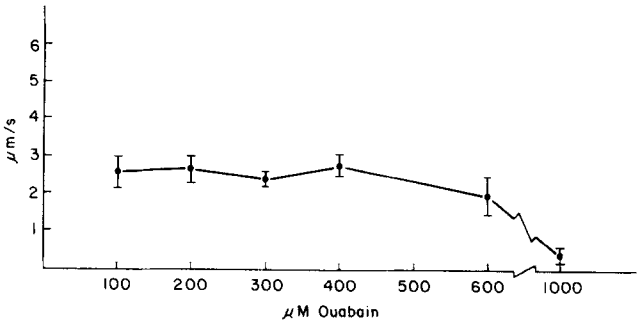

FIGURE 2 Ouabain sensitivity of transport in permeabilized erythrophores. Ouabain did not affect transport rates at 100 to 600 μM levels tested but stopped motion irreversibly, presumably as a result of toxic effects, at 1 mM.

TABLE I

Permeabilization Solution

Digitonin	0.001%
PEG 6000	1.3%
Hank's Balanced Salt Solution	*
PIPES	33 mM
$MgCl_2$	2 mM
EGTA	2 mM
ATP	1 mM
Caffeine	2.5 mM
Aprotinin (proteolytic inhibitor)	0.1%
pH	7.2

* HBSS is diluted to ⅔ normal concentration, and Ca^{2+} is added to make the final free Ca^{2+} concentration 10^{-7} M. Osmolarity is ~235 mOsm.

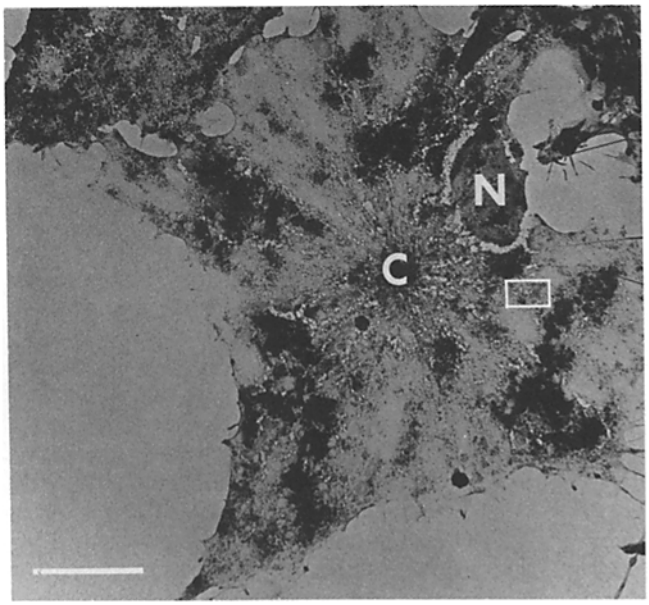

FIGURE 3 HVEM low magnification image of a whole cell permeabilized with 0.001% digitonin for 30 min at 23°C. The cell was metal coated with Pd/Au to reveal holes in the plasma membrane. Centroplast (*C*); Nucleus (*N*). Bar, 10 μM. × 1,400.

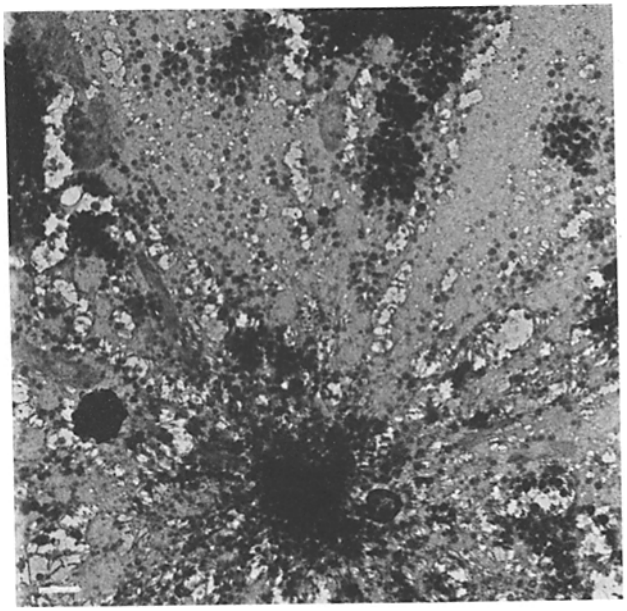

FIGURE 4 Illustration of the extent of permeabilization in the cell in Fig. 3. Note that there are numerous small holes as well as some larger ones distributed in an irregular pattern on the cell surface. Bar, 1.0 μM. × 5,900.

that the plasma membrane surface of intact cells is normally smooth in contour.

The gentle and gradual exchange of solutions is important in these experiments to ensure that a reasonably intact, yet permeabilized plasma membrane is retained. Under these conditions, 100% of the cells are routinely found by scanning electron microscopy (SEM) and HVEM to be punctured and 100% of the cells also remain competent to move their pigment for at least 2 to 3 h. The rapid exchange of cell growth medium with detergent solutions inevitably produces cell lysis, thereby stopping transport and resulting in pigment granule release. It is possible to use digitonin levels reduced to 0.0001% and still obtain permeabilized cells, but all the results reported here are with 0.001% digitonin, since at 0.001% levels the extent of permeabilization and cell extraction remains constant for 2 to 3 h.

To stabilize cytoskeletal elements (microtubules, microtrabeculae) against possible fluctuations and disruptive effects of pH or Ca^{2+} ion levels during permeabilization steps, HBSS containing PIPES (Good Buffer), PEG, EGTA, and Mg^{2+}/ATP is used. A pH range of 6.8 to 7.2 was optimal for the maintenance of transport (Fig. 8) and a pH of 7.2 was used in most of the experiments described.

HVEM Studies

HVEM images show that cells permeabilized under the above conditions retain their normal shape and much of their cytoskeletal morphology (see Figs. 3 and 9). Stereo pictures printed at high magnification demonstrate that microtubules and cross-linking microtrabecular lattice filaments are still present in these cell models in an arrangement similar to that of intact cells (compare Fig. 9 with Fig. 3 *b* in Luby and Porter [20]). In areas where large amounts of the plasma membrane is removed, most of the microtubules and lattice are also removed (Figs. 5 and 9). After metal coating of cells with Pd/Au, areas where the plasma membrane is removed, can easily be identified and the lack of internal structure is apparent in these images, even at low magnifications (see Figs. 4 and 5). Note that some of the holes are much larger than others, especially near the cell center, possibly a result of tearing of the digitonin weakened membrane. We do not believe that any resealing of the holes takes place by fusion of the upper and lower plasma membrane surfaces, although regions where these membranes are closely juxtaposed (i.e., in filopodia), appear less susceptible to digitonin's effects.

Untreated control cells which are directly fixed in glutaraldehyde are prepared during each experiment (Figs. 6 and 7). Although 100% of the cells exposed to digitonin are punctured, the controls exhibited only occasional small holes in their membrane (Fig. 7).

Antibody Studies

Figs. 10 and 12 demonstrate that radially arrayed microtubules and some centrosomal material are labeled when tubulin or HMW-MAPs antibodies are included in the permeabilization solutions for 30 min at 23°C. Time-lapse cine records of cell(s) incubated in the presence of antibody show that the binding of either HMW-MAPs or tubulin antibodies to micro-

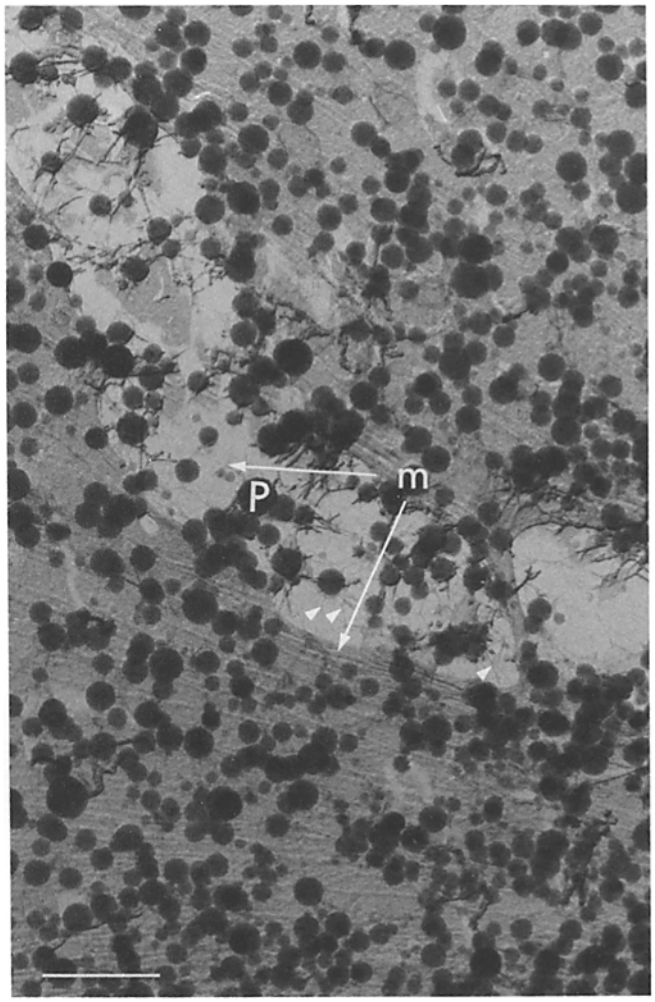

FIGURE 5 High magnification view of part of the cell outlined in Fig. 3. Microtubules (*m*), pigment (*P*), and cross-linking lattice filaments (arrows) are largely removed from subplasmalemmel regions subjacent to where the membrane is removed by digitonin. The upper and lower membranes remain distinct and do not seem to fuse during permeabilization. Bar, 1.0 μM. × 20,000.

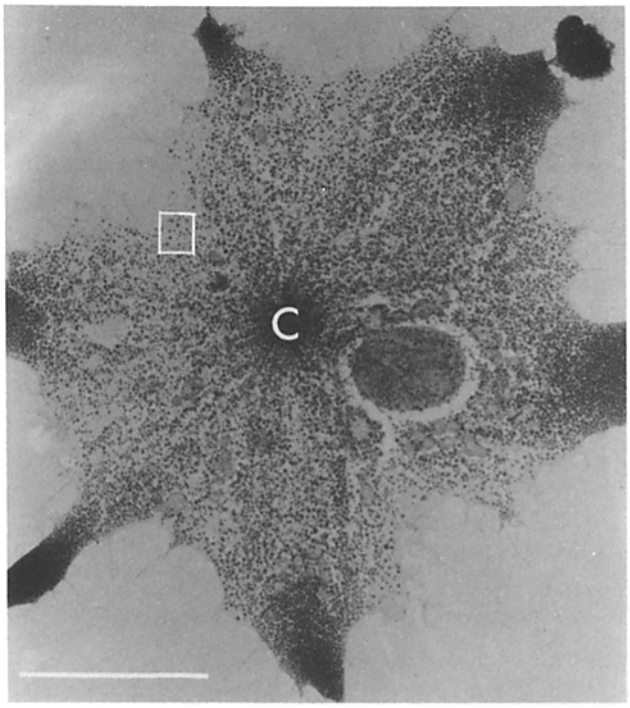

FIGURE 6 HVEM image of a nonpermeabilized cell fixed with its pigment in the dispersed state. The cell consists of a centralized centroplast (*C*) towards which pigment granules normally aggregate and disperse in radial arrays. Bar, 10 μM. × 2,400.

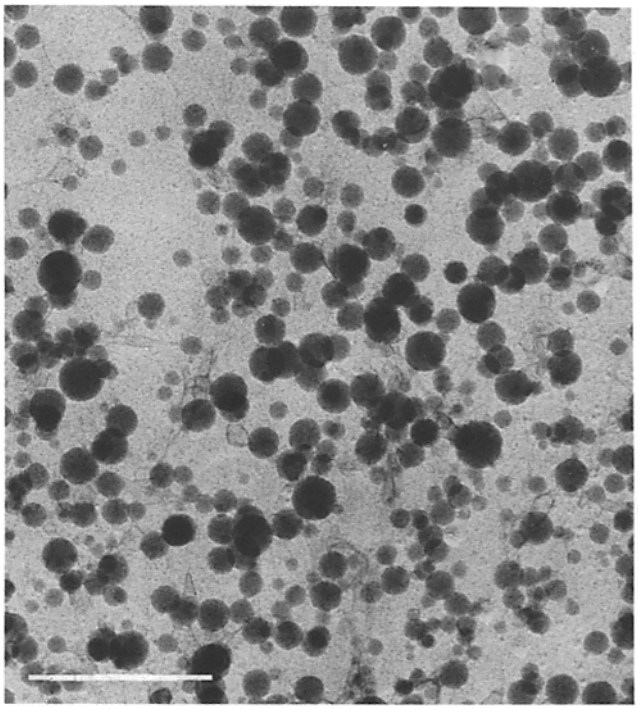

FIGURE 7 High magnification view of the area outline in Fig. 6. The cell was lightly coated with Pd/Au to demonstrate that the cell surface is normally smooth in contour. Pigment granules are visible beneath the plasma membrane but other structures are obscured by the Pd/Au. Bar, 1.0 μM. × 23,000.

tubule structures did not interfere with or prevent saltatory transport (see below). The presence of antibody was subsequently demonstrated by fixing the cells with methanol and secondary labeling with FITC-IgG. In control studies where digitonin was omitted from the solutions tubulin and MAPs antibodies did not enter the cells as demonstrated by a lack of microtubule staining. (Fig. 11).

One critical problem arising with the interpretation of the antibody labeling studies is the existence of red autofluorescent pigment granules in intact cells (Fig. 13) and to a lesser extent in methanol extracted cells (Fig. 11). Often the extracted cells contain no pigment at all and this is the reason for our resorting to methanol fixation to visualize the antibodies rather than simply examining live cells for the presence of tubulin antibody bound to FITC-IgG. Admittedly, Fig. 13 is an extreme example of the problem.

In attempts to overcome this difficulty and visualize antibodies in live, functional cells, we very recently (at the suggestion of Dr. J. Bryan, Baylor College of Medicine) used Rhodamine Isothiocyanate (RITC) coupled to IgG as a fluorochrome probe. The pigment granules emit very little light at fluorescent wavelengths used for RITC (Fig. 14*a*). Fig. 14*a* is of a live, intact cell imaged on the fluorescent microscope using filters for RITC. The same cell is shown in a phase-contrast picture in Fig. 14*b* after permeabilization with digitonin (10 μg/ml), incubation in the presence of tubulin antibody (1:10 dilution) for 30 min, washing with fresh buffer, incubation in RITC-IgG for 30 min, and washing (all in the presence of digitonin). The treatments did not affect the cells basic shape or behavior. Reexamination of the cell with the fluorescent microscope shows that the antibodies (tubulin and RITC-IgG) invade the cell, binding to radially arrayed structures (presumably microtubules) as well as staining diffuse cytoplasmic material (presumably tubulin). Comparison of Figs. 10, 12, and 18 with 14*c* indicates that the diffusely staining material (Fig. *b*) is probably removed during methanol treatments. Control studies using RITC-IgG alone did not produce staining, indicating that the staining pattern observed in Fig. 14*c* is a result of tubulin antibody binding. Some specificity of staining is indicated by the distinct lack of label associated with the nucleus and the central zone of the centrosomal structure (arrowheads).

Time-lapse studies have consistently demonstrated that tubulin and HMW-MAPs antibodies do not effect saltatory transport in erythrophores (Figs. 10 and 12). Similarly, during the course of the experiment described in Fig. 14, tubulin antibody and RITC-IgG did not inhibit motion. Fig. 14*e–g* show that many of the granules are saltating bidirectionally along radial pathways emanating from the cell center in the antibody-labeled cell. Many granules exhibit no apparent motion in the 6-s sequence shown. ~50% of these granules are frozen in place as a result of UV damage during epifluorescent imaging of the cell.

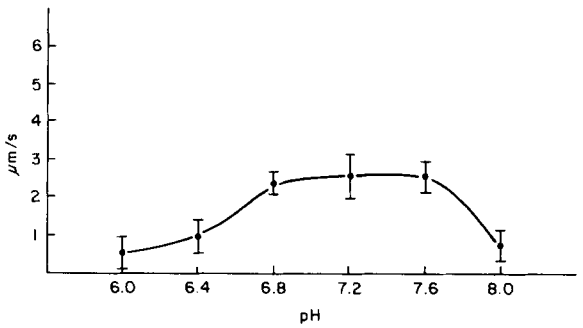

FIGURE 8 The pH dependency of pigment transport at 23°C. Transport rates are optimal at a pH of 6.8 to 7.6. Bars represent rates ± SE.

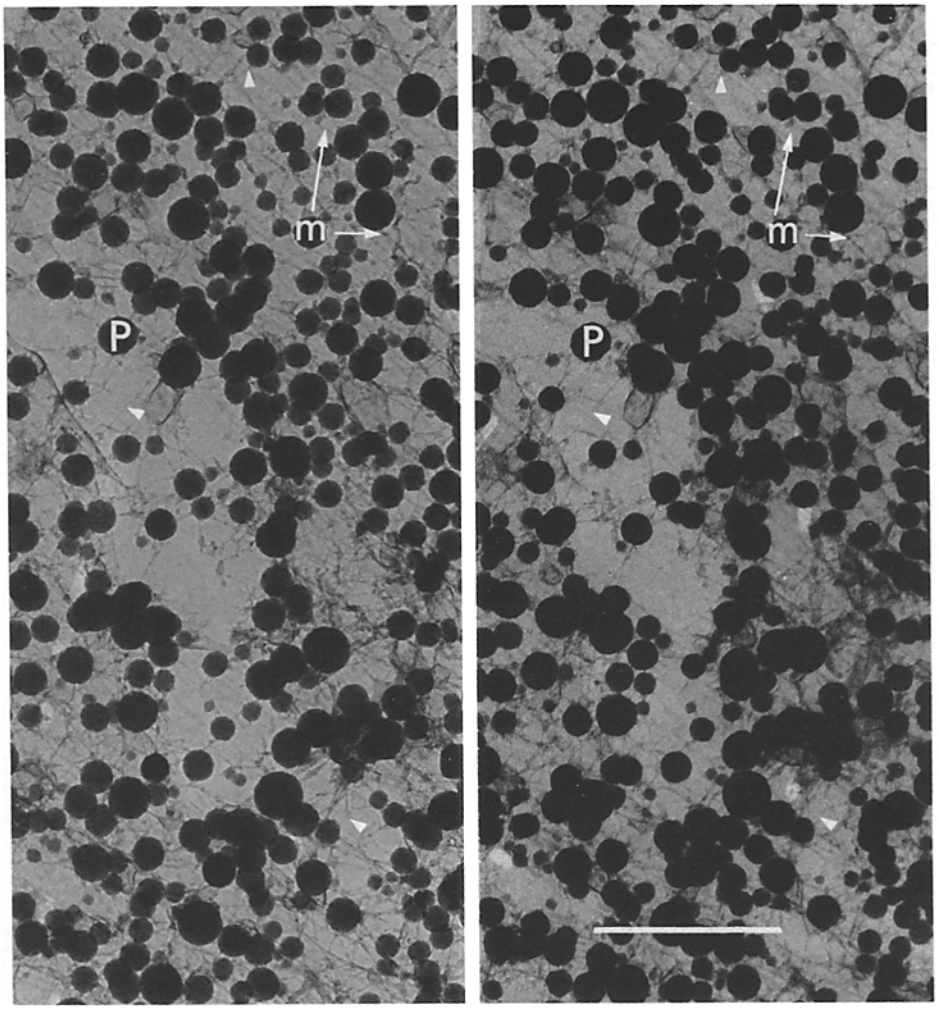

FIGURE 9 High magnification stereo view showing a part of the permeabilized cell shown in Figs. 3 to 5 before being coated with Pd/Au. The pigment (*P*), microtubules (*m*), and the cross-linking microtrabecular lattice filaments (arrows) are maintained relatively intact except in areas where the membrane is removed. Note that pieces of SER are visible in the cytoplasm. These cells are completely unstained except for brief OsO_4. Bar, 1.0 μM. × 25,000.

Calcium Studies

Table II shows that, after exposure of the permeated cells to different Ca^{2+}/EGTA solutions, calcium concentrations for the continuation of transport fall in the range of 0.1 to 0.5 μM. Transport stops by ~10 min in all the cells examined when Ca^{2+} levels are raised above 1 μM or reduced below 0.01 μM. Transport is reinitiated after 10 min in cells exposed to 0.01 μM Ca, if Ca is increased to 0.1 μM levels. We have been unable to restart transport in those cells exposed to Ca^{2+} concentrations >1 μM. In all these studies the omission of Mg^{2+}/ATP from the reactivation solutions usually did not affect the ability of the cell to reinitiate pigment motion by 60 min, although the addition of 2 mM EDTA in Mg^{2+}-free solutions did inhibit the continuation of pigment transport.

Oxidative Phosphorylation Inhibitors

The effects of several specific inhibitors of oxidative phosphorylation are to rapidly inhibit pigment transport in 100% of the cell models. Sodium azide (10 μg/ml) and 2,4 dinitrophenol (2×10^{-5} M) both stopped saltatory motion by 2 to 5 min at 23°C. Table II shows that inhibition is not reversed in reactivation solutions lacking Mg^{2+}/ATP or containing the nonhydrolyzable nucleotide analogues ADP, or AMP-PCP in place of ATP. Inhibition is countered with 1 mM Mg^{2+}/ATP and a gradual recovery of transport occurs by ~10 min at 23°C and by 5 min at 37°C. No recovery occurs at 4°C. Several studies showed that 1 mM ITP, GTP, and UTP will substitute for ATP to promote recovery of transport by ~10 min at 37°C.

In all these studies, the recovery of transport involves an initial stage where short saltations of pigment occur after 2 to 3 min, followed by saltations of longer duration and distance.

Vanadate Effects

Vanadate at concentrations of 0.4 to 10 μM reversibly inhibits saltatory transport in a dose-dependent fashion in 100% of the cells (Figs. 15–17). At the micromolar levels of vanadate tested, particle motion become shorter in duration until it was frozen altogether (with the exception of Brownian motion of some particles). Some localized aggregation of the granules takes place in response to vanadate but for the most part the distribution of pigment is not affected (Fig. 15). Note that there is very little change in cell shape and the pigment does not aggregate to the cell center during experimental treatments. Increasing the pH of solutions to 7.6, near the pka value of vanadate, did enhance the effects of vanadate by decreasing the time required for inhibition of transport (Fig. 16).

Vanadate inhibition is reversed by ~10 min with 1 mM catechol. Frames from time lapse images in Fig. 15 show the effects of vanadate and vanadate reversal with pyrocatechol. After recovery, granule motion and distribution often resembles that observed in freshly permeabilized cells. These experiments can be repeated three or four times before the cells lose their ability to recover. Fig. 15 *c–f* shows that some change in

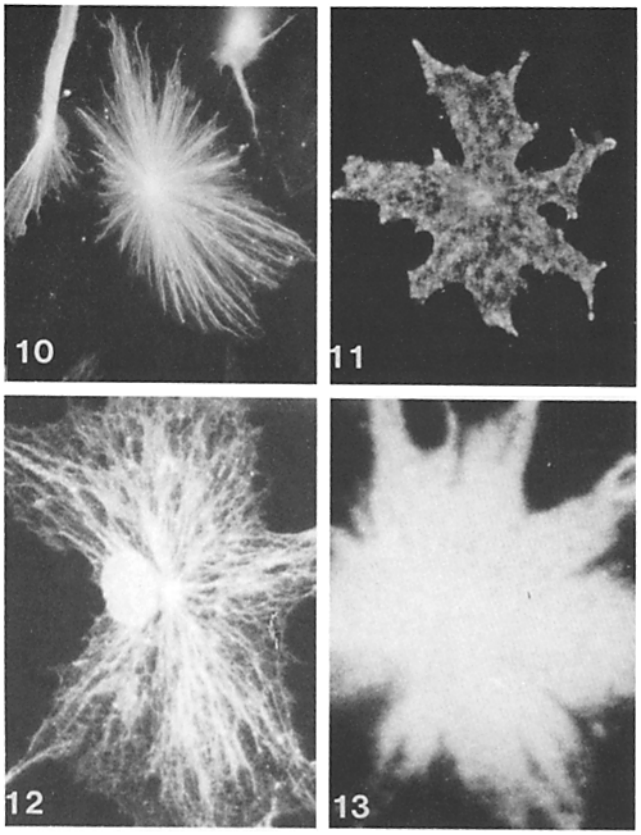

FIGURES 10–13 Indirect immunofluorescence of permeabilized cells incubated with tubulin (Fig. 10) and HMW-MAPs (Fig. 12) antibodies for 30 min at 23°C and then fixed with methanol and stained with GAR-FITC. In both these experiments, transport continued although the microtubule network is bound by the antibodies. Note that some aggregation of microtubules has occurred in Fig. 12 and the nuclear envelope is stained brightly. Fig. 11 shows a non-permeabilized cell incubated with tubulin antibody and fixed with methanol. Fig. 13 shows a cell photographed live with a fluorescent microscope equipped with fluorescein filters (495 nm). Normally, red autofluorescent pigment granules are removed during methanol fixation steps (20) but the bright images in Figs. 11 and 13 are produced by the red pigment. Figs. 10 and 11, × 2,000. Figs. 12 and 13, × 2,900.

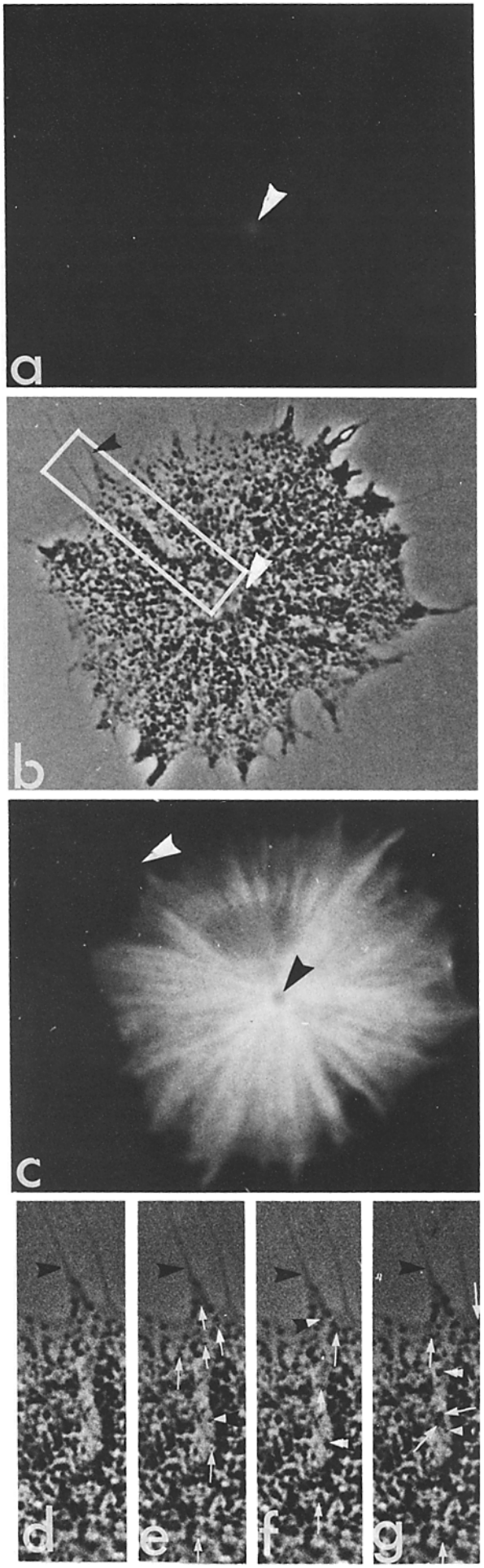

FIGURE 14 Light microscopy images of a chromatophore permeabilized in the presence of tubulin antibody. (*a*) a fluorescent image showing that pigment granules in the untreated cell do not autofluoresce at UV. wavelengths selective for the fluorochrome rhodamine. (*b*) a phase-contrast picture of the erythrophore after 10-min exposure to 10 μg/ml digitonin. The cell's shape is not affected except for some arborization of the filopodia. (*c*) a fluorescent image of the cell in *b* taken after incubation in the presence of tubulin antibody (30 min at 23°C), washing 3 times, exposure to secondary antibody coupled to rhodamine isothiocyanate (RITC), then again washing 3 times and photographing. The image shows that tubulin antibody has entered the permeabilized cell and bound radially arrayed microtubules. A considerable amount of diffuse staining of cytoplasmic tubulin is visible also. (*a–c*) large arrowheads mark the cell center and a filopia. The area outlined in *b* is shown at higher magnification in *d–g*, and *d* is an enlargement of *b*. *e–g* demonstrate that granule motion continues after incubation in permeabilization buffer containing 1° then 2° antibody (pictures are taken at 2-s intervals). Single white arrowheads mark the motion of one granule seen in *e* and *f* and double white arrowheads mark the motion of a second granule seen in *f* and *g* at different positions. Other granules whose motion could not be traced are marked with white arrows. Black arrowheads mark the filopodia seen in *b*. (*a–c*) × 3,000. (*d–g*) × 4,500.

TABLE II

Calcium Effects on Saltatory Motion

[Ca] M	Saltatory motion	Recovery
		10 min
1×10^{-8}	−	+
1×10^{-7}	+ (*3 to 5 μm/s*)	—
5×10^{-7}	+	—
1×10^{-6}	−	+
5×10^{-5}	−	—
1×10^{-4}	−	—

The effects of increasing free Ca^{2+} levels on saltatory transport in permeabilized cells. + denotes that transport continues or is rescued; − indicates that transport stops. Recovery of saltatory transport from Ca^{2+} treatments was monitored in permeabilization solutions containing 10^{-7} M Ca^{2+}

TABLE III

Effects of Nucleotides on Stimulating Recovery of Transport in Na Azide Treated Cells

Nucleotide	Extent of transport observed
1 mM	
Control	++++ (*3 to 5 μm/s*)
No ATP	−
ATP	++++
ADP	−
AMP-PCP	−
GTP	++ (*1 to 3 μm/s*)
ITP	+++ (*3 to 4 μm/s*)
UTP	++

+ Indicates relative amount of transport observed, as determined qualitatively from time-lapse records after 10-min incubation. The rates and amounts of particle motion varied widely during these early stages of recovery and the extent was therefore assessed by qualitative means.
− Indicates little or no transport.

cell shape and pigment distribution (see area outlined) occurs as a result of the saltatory motion. Some particles remain in place and some move in a sporadic fashion but most exhibit normal saltations to and from the cell center (compare Fig. 15 *a* and *b* with *d–f*). In denser areas the motion of granules cannot be readily followed.

Fig. 17 charts the reaction of transport in a single cell during the course of permeabilization, vanadate inhibition, and recovery. The recovery time in these studies is reduced to 5 min from 10 min when 1 mM ATP, UTP, or ITP is added to recovery solutions, but 1 mM ADP or AMP-PCP did not decrease the time significantly. Also, the amount of recovery is improved if the temperature is increased to 37°C in comparison to recovery at 23°C (Fig. 17). Control studies in nonpermeabilized cells show that pigment motion is not affected by vanadate (10–100 μM levels).

In addition to directly inhibiting transport mechanisms, vanadate treatments also have some anomalous effects on microtubule stability. We initially observed that when 1 mM ATP is added to solutions, vanadate levels >4 μM are required to inhibit pigment motion. Studies of time-lapse cine images taken of vanadate (2 μM) treatments in the absence of ATP, show that granule motion in the peripheral cell margins often becomes disoriented, and granules move in many different directions across the radial axis of cells (not shown) before inhibition of transport occurs. Tubulin antibody staining patterns in Fig. 18 demonstrate that these cells suffer from a loss (disassembly) of their normal complement of microtubules (compare Fig. 18 *a* with *c*). 1 mM GTP or ATP (Fig. 18) will prevent this disassembly effect, especially at the lower levels of vanadate tested (< 2 μM), but 1 mM ADP and 1 mM AMP-PCP did not interfere with microtubule disassembly in 2-μM vanadate. Alternatively, increased Mg^{2+} ion levels of 10 mM also stabilized the microtubules against vanadate and at the same time did not interfere with vanadate's ability to inhibit transport. Thus, where microtubule disassembly has occurred, recovery in part involves the reassembly of microtubules. Fig. 18 shows that, after 2-μM vanadate treatment for 10 min in the absence of ATP, the reincubation of these cells in recovery solutions containing 1 mM ATP or GTP produces a full complement of microtubules arranged in their normal radial pattern. Note that microtubule reassembly will occur in the absence of added ATP or GTP but the recovery time is approximately doubled (see discussion below).

NEM and Cytochalasin B and D Effects

In determining the role of actin microfilaments in transport, permeabilization solutions containing 4, 6, and 12 mM NEM were tested for 20 min at 23°C in the presence and absence of 1 mM ATP. We found that cells exposed to NEM did not demonstrate recognizable changes in their behavior. Similarly, addition of 0.1 μg/ml and 10 μg/ml levels of cytochalasins tended to cause an invagination of the cell margins, but this event had no direct effect on the transport of pigment.

DISCUSSION

We report procedures for making functional cell models using the steroid glycoside, digitonin, to permeabilize erythrophores in cytoskeleton-stabilizing solutions. This report represents the first demonstration of detergent-permeabilized cells which can function in saltatory transport, although Cande and colleagues (6, 7) have earlier shown that mitotic spindles lysed with Brij-58 at anaphase will continue to move their chromosomes to the poles and undergo cleavage.

There are several possible reasons why the digitonin cell models retain an ability to function in vitro. Most important is that digitonin preferentially binds cholesterol and other B-hydroxysterols (28), and it is thought to intercalate into the membrane, weaken its structure and thereby cause vesiculation in fragile regions of the plasma membrane. With the removal of membrane, numerous holes subsequently appear in the cell surface in 100% of the cells. Because of the high molar ratio of cholesterol to phospholipids (1:4) in the plasma membrane and the low levels of cholesterol (<3%) in other membranes (mitochondrial, endoplasmic reticulum, and lysosomal), the plasma membrane is selectively permeabilized with digitonin, without loss or impairment of the normal morphology of most organelles (9). We believe therefore, that a minimal disruption of intracellular structures and associated membrane material occurs during permeabilization as a result of the reduced digitonin levels (0.001%) used. Consequently, cytoskeletal structural components and cytosolic proteins important for transport are also retained under these mild conditions (Fig. 9). We have found that when higher levels of digitonin (>0.001%) are used, or if cells are rapidly flushed with the permeabilization solutions, all the plasma membrane is removed, cell lysis results, and pigment granules are released. Even under such severe lysis conditions, however, mitochondrial, endoplasmic reticulum, and lysosomal membranes, plus some cytosolic proteins, are still retained along with the cytoskeleton (unpublished results). Thus, digitonin provides a unique advantage over other commonly used agents such as Triton, Brij-58, or glycerol as these agents are relatively nonspecific in their effects on membranes and cytosolic proteins,

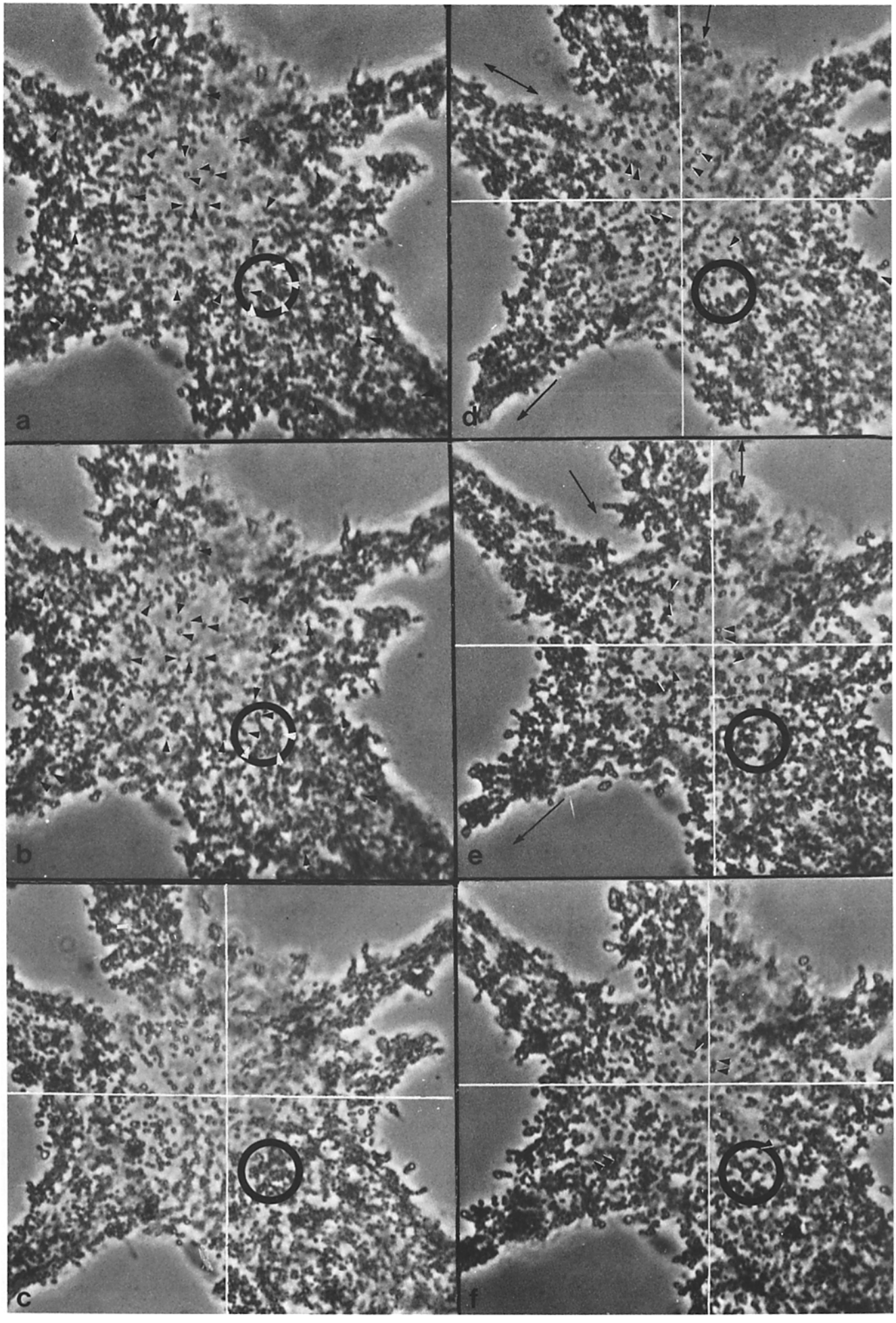
a
b
c
d
e
f

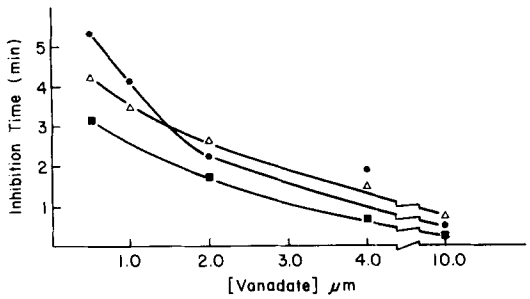

FIGURE 16 Graph showing vanadate inhibition of transport at different pHs. Increasing the concentration of vanadate from 0.4 to 10 μM reduces the time of complete inhibition of transport from ~5 min to 30 s at pH 7.2 (●). At pH 6.4 (△) there is little change in the times required for stopping transport, but at pH 7.8 (■), near the pK_a value of vanadate, decreases the inhibition time to some extent. 0.1 mM ATP is included in the solutions used.

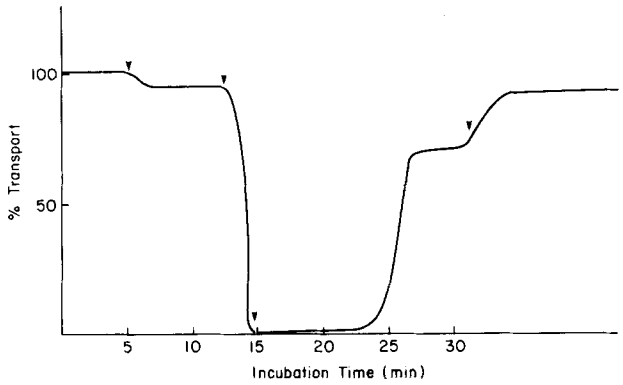

FIGURE 17 Graph made from time-lapse observations showing inhibition by vanadate and reversal of vanadate effects. Cells exposed to 0.001% digitonin at 23°C at 5 min (first arrow) show some reduction of transport and motion is stopped completely by 15 min with 10 μM vanadate added at 12 min (second arrow). Addition of 1 mM catechol at 15 min (third arrow) reverses vanadate's effects by ~10 min at 23°C. Increasing the temperature to 37°C (fourth arrow) restores transport to levels approaching that of intact cells.

and generally have a disruptive effects on intracellular motion in cultured cells (unpublished results).

Calcium Requirements for Transport

From in vivo work using ionophores, shifts in free Ca ion levels are proposed to regulate saltatory transport along microtubule structures (33). In this paper, the use of cell models has eliminated the necessity of using ionophores which may have nonspecific effects influencing the behavior of cells. We have found that pigment transport continues after permeabilization at concentrations of 0.1 to 0.5 μM Ca, but is discontinued at levels below 0.01 μM. In addition, a maximum Ca^{2+} level exists for pigment translocations in vitro (1.0 μM) above which motion initially becomes random in the peripheral margins, and then gradually stops. Unfortunately this motion is not reinstated when Ca^{2+} levels are reduced, perhaps due to microtubule disruption or Ca^{2+}-triggered contractions of microtrabecular lattice components (33). In this regard, Schliwa, et al. (31) have recently found that micromolar amounts of Ca^{2+} will cause microtubule disassembly from their distal ends in lysed cells. Thus, an irreversible microtubule disassembly could conceivably occur in response to increased Ca^{2+}, and this in conjunction with contraction events could be sufficient to stop transport. Further correlative HVEM and immunofluorescent images will help resolve this question.

The data generally indicate that large amounts or large increases in intracellular Ca^{2+} are not required for the continuation of saltatory motion. This result is similar to recent in vitro data of others showing that the activation of cilia or flagella beating in vitro requires little Ca^{2+} (3) (~1 μM), and that increases in Ca^{2+} ions are not necessary for furrowing

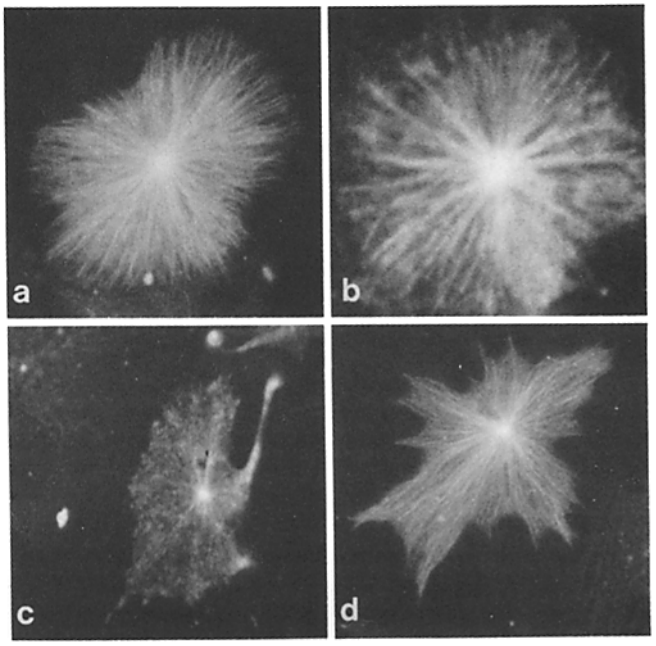

FIGURE 18 Tubulin antibody-labeled fluorescent images of permeabilized erythrophores treated for 5 min with solutions containing (*a*) 1 mM ATP, no vanadate; (*b*) 10 μM vanadate plus 1 mM ATP; (*c*) 2 μM vanadate, with no ATP added; (*d*) 1 mM ATP for 5 min after exposure to solution (*c*). Note that a full complement of microtubules is present in cells which are not exposed to vanadate, or are allowed to recover from vanadate in ATP-containing solutions. Cells exposed to excess vanadate (10 μM) still retain some microtubules if ATP is included in the solution. In the absence of ATP, vanadate induces microtubule disassembly before and during the inhibition of transport activities. × 2,000.

FIGURE 15 Phase contrast cine images showing the effects of vanadate (5 μM) on permeabilized erythrophores. *a* and *b* are taken 30 s apart after exposure to vanadate for 5 min. All linearly directed motion was discontinued and as a result numerous granules (arrowheads) can now be found in the same spot in *a* and *b* (see encircled area). The changes in overall pigment distribution are due to brownian motions moving some granules in and out of the plane of focus. *c–f* show recovery of saltatory transport with the addition of 1 mM pyrocatechol to solutions. *c* is after 5-min recovery and *d–f* are taken at 2-s intervals after 10-min recovery. The linear motion of some of the granules (arrowheads) can be followed by progressing from *d* to *f* where the same granules are marked with arrowheads. Arrows mark the direction of motion in *d* and *e* for each quadrant. Dramatic changes in pigment distribution and some changes in cell shape occur as a result of the saltatory events (see area encircled). Note that motion is to-and-from the cell center where the quadrants intersect. × 2,500.

activity in lysed mitotic spindles (5), or for cytoplasmic contractions in glycerinated pigmented epithelium (24). In contrast, in smooth muscle and striated muscle, motility is induced by small increases (to 1 μM) in Ca^{2+} (14, 15, and 19) from a free Ca^{2+} level of 0.05 to 0.10 μM in unstimulated muscle. Increased Ca^{2+} levels are also known to trigger contractions of gelled cytoplasmic extracts (10, 35).

Our results are dissimilar from observations by Luby (20) on intact cells where she showed that higher Ca^{2+} levels of 5×10^{-6} M were required to cause an aggregation of pigment. In Luby's work, Ca^{2+} and ionophore are probably affecting both membrane and cytoskeletal related events to produce their effect, whereas in our system, the Ca^{2+} is interacting directly with cytoskeletal components to influence their behavior.

So far we have been unable to duplicate Luby's in vivo observations on permeabilized cells. In the presence of caffeine (2.5 mM) the cells do not aggregate their pigment to the cell center in response to high Ca^{2+} levels ($>10^{-6}$ M). With the removal of caffeine from solutions, the cells can aggregate their pigment irreversibly even in the presence of reduced Ca^{2+} levels (10^{-8} M). We propose that higher Ca^{2+} levels serve to trigger wholesale contractions of the microtrabecular lattice that mediate pigment aggregation, while reduced Ca^{2+} levels as well as smaller shifts in Ca^{2+} modulate the saltation events in dispersed cells. We are currently attempting to develop permeabilization solutions that permit the cyclic pulsing of pigment granules to and from the cell center.

Oxidative Phosphorylation Inhibitors

In this paper we have used cell models to investigate the importance of ATP for saltatory movements in caffeine-dispersed cells. The results show that pigment motion is temperature- and ATP-dependent. Inhibition of cellular ATP supplies using metabolic inhibitors or reduction of temperatures to 4°C causes a rapid termination of motion in 100% of the cells. This effect is completely reversible with ATP and increased temperatures, indicating a direct dependence of transport on ATP supplies. The ability of EDTA to inhibit recovery further indicates that Mg^{2+}-ATP is important in motion. This information is in agreement with recent in vivo observations of Luby and Porter (21) showing that oxidative phosphorylation inhibitors can gradually inhibit energy-dependent steps important for pigment redispersion. We do not understand the molecular mechanism of ATP action but one possibility is that ATP provides energy for ATPase-mediated processes such as shifting Ca^{2+} levels important in the regulation of molecular events (i.e., contractions and expansions of the microtrabecular lattice). Alternatively, microtubule-associated, dynein ATPase-driven motility events exhibit a direct dependence on ATP supplies in cilia and flagella (17) and similar ATPases may be involved in pigment motion as discussed below.

Vanadate Effects

The results demonstrate that vanadate can reversibly inhibit pigment motion in erythrophores. The significance of this evidence is not entirely clear, but we believe that a vanadate-sensitive dyneinlike ATPase is important for saltatory transport in these cells. In support of this interpretation is evidence by others that micromolar amounts of vanadate in the +5 oxidation state can reversibly inhibit dynein-ATPases (17), but does not inhibit actomyosin ATPase, F1 ATPase from mitochondria, or the Ca-ATPase from sarcoplasmic reticulum (8). More importantly, vanadate prevents the beating of flagella and cilia (5, 17), stops anaphase movement of chromosomes, and inhibits spindle elongation in PtK_1 cells (6, 7). Taken together, these results suggest that a microtubule-linked dynein mechanochemical system could conceivably exist in all microtubule-directed motility systems. Sakai, et al. (27) has demonstrated that chromosome movement is blocked by antibodies raised against dynein, indicating a direct role for dynein ATPases in this type of transport. Thus, the structural integration of dynein into the microtubule associated-microtrabecular lattice component may mediate at least some phases of granule motion in erythrophores.

We cannot rule out the possibility that vanadate may also inhibit transport, at least in part, by affecting activities in addition to a dynein-ATPase. At the level of vanadate tested (2 μM) we found that 1 mM ATP is needed to maintain the structural integrity of the cytoskeleton and transport. The removal of ATP from solutions at these concentrations of vanadate results in microtubule disassembly and a rapid inhibition of transport. We suggest, therefore, that vanadate also has nonspecific disruptive effects on cytoskeletal elements, perhaps by interfering with ATPase synthesis, and indirectly with nucleotide hydrolysis for the maintenance of energy levels in the cell. In part, this might explain why nucleotides and Mg^{2+} ions can counter the effects of vanadate on microtubules since both promote the assembly and the stability of microtubules. This interpretation is supported by in vitro observations of Cande and Wolniak (7) showing microtubule assembly is not affected by vanadate.

One interesting aspect of this work is that free tubulin protein from microtubule disassembly does not appear to diffuse out of the cell during the exposure of cells to vanadate. Microtubules are rapidly reassembled after the removal or reduction of vanadate, presumably from the same subunits. The intriguing question which arises is whether tubulin subunits or protomers of tubulin are temporally incorporated into the lattice for the reassembly of microtubules when favorable conditions occur (studies in progress).

Ouabain Effects

Intact erythrophores respond to ouabain and rapidly aggregate their pigment, indicating that membrane-bound Na^+/K^+ ATPases can regulate pigment translocations, at least in cultured cells. Because these cells are rendered insensitive to ouabain effects during permeabilization steps, we believe that the holes made in the plasma membrane must permit the free exchange of ions, thus eliminating membrane potential effects on transport events. The fact that antibodies, vanadate, and Ca^{2+} will rapidly enter into permeabilized cells confirms this notion of free exchange taking place. More importantly, the ability of transport to continue in detergent- and ouabain-treated cells indicates that intracellular Na^+/K^+ ATPases are not important for saltatory motion. In support of the above suggestion, Cantley, et al. (8) have demonstrated that vanadate normally stops ouabain-sensitive Na^+/K^+ ATPases and that this effect is enhanced with increased Mg^{2+} ion levels of 20 mM. Our results show that vanadate is not enhanced in its action by Mg^{2+}, again indicating that a Na^+/K^+ ATPase is unimportant for pigment saltations.

Our inability to reverse the aggregating effects of 100 mM KCl in the permeabilized system may reflect an involvement of the plasma membrane Na^+/K^+ ATPases and Na^+/K^+ balances in various stages of this phenomenon (pigment disper-

sion). Why KCl can induce aggregation in permeabilized cells in the first place is unclear, unless KCl-triggered changes in related membrane-lattice interactions can still occur. The effects of KCl and caffeine deserve more attention. Both may have an effect on intracellular membrane compartments, like mitochondria or ER, in addition to the lattice. Caffeine is known to inhibit phosphodiesterase and indirectly raise cAMP levels. In addition, caffeine can induce a localized leakage of Ca^{2+} from intracellular membrane compartments.

NEM has been shown to inhibit myosin ATPases and the contraction of actomyosin in the presence of Mg^{2+}/ATP while cytochalasins B and D disrupt actin filaments and actin latticeworks to interfere with actin-dependent motility. Neither NEM nor cytochalasin B or D has a striking effect on the continuation of transport in permeabilized cells. In the presence of NEM granule transport continues uninterrupted for hours and at increased cytochalasin levels (1 μg/ml) (30 min or longer), some arborization of the cell margins occurs but there is no direct interference with transport. This occurs because the cell margins contain an actin network for ruffling and this is eventually dissolved in the presence of cytochalasins (unpublished immunofluorescence results). Taking these results, in conjunction with the vanadate data, we conclude that actin and myosin are not involved in the saltatory phase of pigment motion in dispersed cells. Of course, we cannot rule out the possible importance of actomyosin or microfilaments in stages of nonsaltatory pigment aggregation.

Summary

In conclusion, we have demonstrated that it is possible to make functional cell models for monitoring saltatory transport. By changing the composition of the permeabilization solution we can speed up, slow down, stop (freeze), and reinitiate saltatory transport. Using these detergent cell models, it is now feasible to further examine the regulatory role of Ca^{2+}, Mg^{2+}, phosphorylation, and other possible factors in saltatory transport. We intend to carry out HVEM analyses of the effects of these agents on cell structure and related functions to evaluate the role of organizational changes in the microtrabecular lattice in organelle transport.

Several preliminary reports of saltatory transport by ourselves and others were presented at the 21st American Society for Cell Biology Meetings (Nov. 1981). Dr. David Forman has kindly provided us with a preprint of his paper submitted to Exp. Cell Res. (now in press) showing that vanadate inhibits saltatory movement in Brij-58-permeabilized fibroblasts. In support of the work reported here, M. Beckerle and K. R. Porter (2) have recently reported observations on microinjected erythrophores showing that the dynein ATPase inhibitors, vanadate and EHNA, will inhibit granule transport in intact cells.

We wish to thank Dr. Keith Porter for allowing us the opportunity to pursue topics of our choosing while in his laboratory. We also express our thanks to George Wray for this assistance with the HVEM.

Supported by Muscular Dystrophy PDF's to M. E. Stearns (Canadian) and R. L. Ochs (U. S. A.) and a MDA grant to Keith Porter.

Received for publication 16 October 1981, and in revised form 17 May 1982.

REFERENCES

1. Beckerle, M. C., H. R. Byers, K. Fujiwara, and K. R. Porter. 1979. Indirect immunofluorescent and stereo high voltage electron microscopy evidence for microtubule-associated migration of pigment granules in erythrophores. *J. Cell Biol.* 83(2, Pt. 2):352*a*(Abstr.).
2. Beckerle, M., and K. R. Porter. 1982. Inhibitors of dynein activity block intracellular transport in erythrophores. *Nature (Lond.).* 295:701–703.
3. Bessen, M. R., R. B. Fay, and G. B. Witman. 1980. Calcium control of waveform in isolated flagellar axonemes of *Chlamydomonas. J. Cell Biol.* 86:446–455.
4. Byers, H. R., and K. R. Porter. 1977. Transformations in the structure of the cytoplasmic ground substance in erythrophores during pigment aggregation and dispersion. I. A study using whole cell preparations in stereo high voltage electron microscopy. *J. Cell Biol.* 75:541–558.
5. Cande, W. Z. 1980. A permeabilized cell model for studying cytokinesis using mammalian tissue culture cells. *J. Cell Biol.* 87:326–335.
6. Cande, W. Z., K. McDonald, and R. L. Meeusen. 1981. A permeabilized cell model for studying cell division: a comparison of anaphase chromosome movement and cleavage furrow constriction in lyzed PtK_1 cells. *J. Cell Biol.* 88:618–629.
7. Cande, W. Z., and S. M. Wolniak. 1978. Chromosome movement in lyzed mitotic cells is inhibited by vanadate. *J. Cell Biol.* 79:573–580.
8. Cantley, L. C., Jr., L. Josephson, R. Warner, M. Yanagisawa, C. Lechene, and G. Guidotti. 1977. Vanadate is a potent (Na, K)-ATPase inhibitor found in ATP derived from muscle. *J. Biol. Chem.* 252:7421–7423.
9. Colbeau, A., J. Nachbaur, and P. A. Vignais. 1971. Enzyme characterization and lipid composition of rat liver subcellular membranes. *Biochim. Biophys. Acta.* 249:462–492.
10. Condeelis, J. S., and D. L. Taylor. 1976. The contractile basis of amoeboid movement. V. The control of gelation, solation, and contraction in extracts from *Dictyostelium discoideum. J. Cell Biol.* 74:901–924.
11. Connolly, J. A., and V. I. Kalnins. 1980. The distribution of tau and HMW microtubule-associated proteins in different cell types. *Exp. Cell Res.* 127:341–350.
12. Connolly, J. A., and V. I. Kalnins. 1980. Tau and HMW microtubule-associated proteins have different microtubule binding sites *in vivo. Eur. J. Cell Biol.* 21:296–300.
13. Connolly, J. A., V. I. Kalnins, D. W. Cleveland, and M. W. Kirschner. 1978. Intracellular localization of the high molecular weight microtubule accessory protein by indirect immunofluorescence. *J. Cell Biol.* 76:781–786.
14. Ebashi, S., M. Endo, and I. Ohtsuki. 1969. Control of muscle contraction. *Quart. Rev. Biophys.* 2:351–384.
15. Filo, R. S., D. F. Bohr, and J. C. Ruegg. 1965. Glycerinated skeletal and smooth muscle calcium and magnesium dependence. *Science (Wash. D. C.).* 147:1581–1584.
16. Fiskum, G., S. W. Craig, G. L. Decker, and A. L. Lehninger. 1980. The cytoskeleton of digitonin-treated rat hepatocytes. *Proc. Natl. Acad. Sci. U. S. A.* 77:3430–3434.
17. Gibbons, I. R., M. P. Cosson, J. A. Evans, G. H. Gibbons, B. Houck, K. H. Martinson, W. S. Sale, and W-J. Y. Tang. 1978. Potent inhibition of dynein adenosine triphosphate and of the motility of cilia and sperm flagella by vanadate. *Proc. Natl. Acad. Sci. U. S. A.* 75:2220–2224.
18. Green, L. 1968. Mechanisms of movement of granules in melanocytes of *Fundulus heteroclitus* (L). *Proc. Natl. Acad. Sci. U. S. A.* 59:1179–1186.
19. Hitchcock, S. E. 1977. Regulation of motility in nonmuscle cells. *J. Cell Biol.* 74:1–15.
20. Luby, K. J. 1980. Both extracellular and intracellular Ca^{2+} play a role in the control of pigment migration in erythrophores of *Holocentrus. Eur. J. Cell Biol.* 22:352*a*(Abstr.).
21. Luby, K. J., and K. R. Porter. 1980. The control of pigment migration in isolated erythrophores of *Holocentrus ascensionis* (Osbeck). I. Energy requirements. *Cell.* 21:13–23.
22. Obika, M., D. G. Menter, T. T. Tchen, and J. D. Taylor. 1978. Actin microfilaments in melanophores of *Fundulus heteroclitus. Cell Tiss. Res.* 193:387–397.
23. Ochs, R. L., and M. E. Stearns. 1981. Colloidal gold immunolabeling of whole-mount erythrophore cytoskeletons: localization of tubulin and HMW-MAPs. *Biol. Cell.* 42:19–28.
24. Owaribe, K., R. Kodama, and G. Eguchi. 1981. Demonstration of contractility of circumferential actin bundles and its morphogenetic significance in pigmented epithelium *in vitro* and *in vivo. J. Cell Biol.* 90:507–514.
25. Porter, K. R. 1976. Introduction: Motility in Cells. *In:* Cell Motility. R. Goldman, T. Pollard, and J. Rosenbarum, editors. Cold Spring Harbor Symposium, Cold Spring Harbor, NY. 1–28.
26. Porter, K. R., and M. A. McNiven. 1982. The cytoplast: a unit structure in chromatophores. *Cell.* In press.
27. Sakai, H., I. Mabuchi, S. Shimoda, R. Kuriyama, K. Ogawa, and H. Mohri. 1976. Induction of chromosome motion in the glycerol isolated mitotic apparatus: nucleotide specificity and effects of antidynein and myosin sera on the motion. *Dev. Growth Diff.* 18:211–219.
28. Scallen, T. J., and A. E. Dietert. 1969. The quantitative retention of cholesterol in mouse liver prepared for electron microscopy by fixation in a digitonin-containing aldehyde solution. *J. Cell Biol.* 40:802–813.
29. Schliwa, M. 1979. Stereo high voltage electron microscopy of melanophores. Matrix transformations during pigment movements and the effects of cold and colchicine. *Exp. Cell Res.* 118:323–340.
30. Schliwa, M., and J. Bereiter-Hahn. 1975. Pigment movements in fish melanophores: morphological and physiological studies. V. Evidence for a microtubule-dependent contractile system. *Cell Tissue Res.* 158:61–73.
31. Schliwa, M., U. Euteneuer, J. C. Bulinski, and J. G. Izant. 1981. Calcium lability of cytoplasmic microtubules and its modulation by microtubule-associated proteins. *Proc. Natl. Acad. Sci. U. S. A.* 78:1037–1041.
32. Schliwa, M., E. Euteneuer, W. Herzog, and K. Weber. 1979. Evidence for rapid structural and functional changes of the melanophore microtubule-organizing center upon pigment movements. *J. Cell Biol.* 83:623–632.
33. Stearns, M. E. 1981. High voltage electron microscopy (HVEM) studies of axoplasmic transport in neurons: a possible regulatory role for divalent cations. *J. Cell Biol.* 92:765–776.
34. Stossel, T. P., and J. H. Hartwig. 1976. Interactions of actin, myosin, and a new actin-binding protein of rabbit pulmonary macrophages. II. Role in cytoplasmic movement and phagocytosis. *J. Cell Biol.* 68:602–619.
35. Taylor, D. L., and J. S. Condeelis. 1979. Cytoplasmic structure and contractility in amoeboid cells. *Int. Rev. Cytol.* 56:57–144.
36. Wikswo, M. A., and R. R. Novales. 1969. The effect of colchicine on migration of pigment granules in the melanophores of *Fundulus heteroclitus. J. Ultrastruct. Res.* 41:189–201.
37. Wolosewick, J. J., and K. R. Porter. 1979. Microtrabecular lattice of the cytoplasmic ground substance. Artifact or reality? *J. Cell Biol.* 82:114–139.